Critical Care

RESEARCH

Open Access

Identification of a robust metabolic signature associated with hospital-acquired pneumonia and response to interferon-gamma treatment in critically ill patients

Melanie Petrier[1], Debajyoti Sinha[1], Florian P. Martin[1,2], Cecile Poulain[1,2], Delphine Flattres Duchaussoy[2], Athanasios Ziogas[3], Boris Novakovic[4], Laura Hurtado-Navarro[3,5], Anaísa V Ferreira[3], Joost H. A. Martens[6], Despoina Koulenti[7,8], Laia Fernández-Barat[9,10,11], Antoni Torres[9], Emmanuel Montassier[1,12], Mihai G. Netea[5,13], Jeremie Poschmann[1†] and Antoine Roquilly[1,2,14*†]

Abstract

Aim Our objective was to increase our understanding of the effects of the time course of metabolic alterations on the risk of hospital-acquired pneumonia (HAP) and response to treatment in critically ill patients.

Methods We first studied the blood metabolome at day 1, day 3-4 and day 6-7 of patients from a prospective, observational cohort of brain-injured patients in two French centres. We classified the metabolic response by unsupervised longitudinal consensus clustering. To evaluate the robustness of metabolic patterns, a Fast-and-Frugal Tree trained on the discovery cohort was applied to a replication dataset from the PREV-HAP randomised clinical trial testing interferon gamma-1b for the prevention of HAP in critically ill patients. The primary outcome was the association of metabolic response patterns with HAP.

Findings Of the 128 patients analysed (330 samples), 57 (45%) had developed HAP and 21 (16%) acute respiratory distress syndrome (ARDS). Based on metabolites involved in fatty acid metabolism, we identified three metabolic response patterns associated with the risks of HAP (24%, 60% and 78% of HAP, respectively) and ARDS (6%, 16% and 43%, respectively). In a replication dataset (315 samples from 105 patients), we found similarities regarding blood metabolite temporal courses and associations with HAP (18%, 28% and 40% of HAP, respectively). Moreover, the probability of being discharged alive from the ICU with interferon gamma-1b was decreased in patients with low-risk metabolic response patterns and increased in patients with high-risk metabolic response patterns.

Conclusions Longitudinal clustering classified metabolic response patterns into low-, moderate-, and high-risk groups for HAP and can help identify responders and non-responders to interferon gamma-1b after a single treatment injection.

†Jeremie Poschmann, Antoine Roquilly lead contacts.

*Correspondence:
Antoine Roquilly
antoine.roquilly@univ-nantes.fr

Full list of author information is available at the end of the article

Trial registration Number clinicaltrial.gov NCT02003196 and NCT04793568
Keywords Pneumonia, Metabolome, Interferon-gamma, Precision medicine

Introduction

Pneumonia is the most frequent cause of hospital-acquired infection, with more than 800,000 episodes of hospital-acquired pneumonia recorded every year in Europe [1, 2]. Despite the publications of guidelines for HAP prevention and treatment, up to 30% of patients hospitalised in intensive care units for more than 48 hours develop HAP [3–5].

Several markers of immunosuppression have been associated in critically ill patients with the risk of developing HAP, and immune-stimulation strategies have been proposed to address this medical concern [6–9]. A placebo-controlled phase II randomised clinical trial testing human recombinant IFNγ treatment to prevent HAP in critically ill patients was discontinued early because the study intervention was associated with pneumonia and severe lung inflammatory responses [10]. Increasing our understanding of the underlying pathophysiology linking critical illness to HAP could help identify responders and non-responders to IFNγ treatment and enable the implementation of precision medicine [11, 12].

Profound immune alterations and microbial dysbiosis have been separately associated with HAP and ARDS in critically ill patients [13–19]. However, these approaches did not achieve the required accuracy for clinical implementation. We and others have proposed that developing robust phenotypes and endotypes associated with respiratory complications and treatment response requires combining immune and microbiome investigations to capture the complete picture of lung host-microbiome interactions [20]. A few monocentric studies have supported this hypothesis [21], but the pathophysiological processes have not been thoroughly investigated.

Issues persist in integrating microbiome and immune datasets, as well as in accounting for longitudinal changes. Circulating metabolites derived from both host and microbiome metabolism can serve as biomarkers of immune dysfunction and microbiome-related alterations in critically ill patients [22]. We hypothesised first that temporal changes in the circulating metabolome during critical illness are associated with the development of HAP, and second that these temporal metabolic patterns are associated with the response to immune interventions for the prevention of HAP. To address this, we conducted a longitudinal, high-throughput analysis of blood metabolome composition in two large prospective cohorts of critically ill patients. We identified distinct metabolic patterns (endotypes) associated with patient outcomes and response to interferon-gamma 1b treatment and proposed plausible pathophysiological mechanisms (metabolic pathways and monocyte epigenetic regulation).

Methods

Study design

We applied high throughput, untargeted, metabolomic analyses on plasma samples collected in an observational discovery cohort (discovery) to discover metabolomic profiles associated with the risk for development of HAP, and on samples from a randomized clinical trial testing interferon gamma for the prevention of HAP (validation) to demonstrate the robustness of these profiles.

Study populations

In the discovery cohort (IBIS cohort), patients were enrolled from 31st January 2017 to 5th May 2020 in two French Surgical Intensive Care Units of one university hospital (Nantes, France) [6, 13]. Inclusion criteria were male or female, 18-80 years old, brain injury (Glasgow Coma Scale below or equal to 12 and abnormal brain-CT scan) and receiving invasive mechanical ventilation (MV). Exclusion criteria were immunosuppressive drugs and pregnancy. Patients from the discovery and validation cohorts were clinically followed up for 90 days.

The validation cohort originated from the PREV-HAP trial, an investigator-initiated multicenter, parallel-group, double-blind, randomized clinical trial performed in 9 French ICUs [10]. Patients aged between 18 and 85 years, receiving invasive mechanical ventilation, with one or more acute organ failures at the time of inclusion, were randomised to interferon gamma-1b (1b (100 µg/0.5 ml vials, IMUKIN®, from Clinigen®) or placebo (normal saline vials). Participants received five subcutaneous injections of 100 µg of recombinant interferon gamma-1b (interferon-gamma group) or matching placebo (placebo group) from day 1 to day 9 (i.e., one injection every 48h).

Controlled healthy samples were collected from matched healthy blood donors recruited at the Blood Transfusion Center (Etablissement Francais du Sang).

Ethical approvals

The collection of human samples within IBIS has been declared to the French Ministry of Health (*Programme de recherche "Immunologie"*, DC2014-2206, authorization renewed DC-2017-2987) and was approved by the *Comité de Protection des Personnes Ouest IV* (7/04/2015 and 08/10/2020, number clinicaltrial.gov NCT02003196). The study was registered the 5th of January 2014 (number clinicaltrial.gov NCT02003196). The CERAR (Ethics Committee for Anesthesiology and Intensive Care

Research) approved this secondary analysis protocol under the reference number IRB 00010254 – 2020 - 041. The PREV-HAP study protocol was approved by the Ouest II Angers (France) Ethics Committee in March 2021. This trial complied with the Declaration of Helsinki and was registered in March 2021 (number clinicaltrial.gov NCT04793568). All patients or their legal representatives consented to the use of data and samples for this study, as appropriate under national legislation.

Primary outcome

Was to identify specific metabolomic profiles associated with the risk for development of HAP. HAP was defined as pneumonia that occurred 48 h after hospitalization and required at least two clinical signs (body temperature >38°C; leucocytosis >12 000 cells per mL, leucopenia <4000 cells per mL, or purulent pulmonary secretions) with the appearance of a new infiltrate or worsening of an existing infiltrate on chest radiography, plus semi-quantitative or quantitative positive respiratory fluid cultures. Respiratory samples were obtained before starting any new antimicrobial therapy for pneumonia. Early- and late-onset HAP were defined as HAP occurring less than five days and five or more days after hospital admission, respectively. Intensivists blindly reviewed HAP and acute respiratory distress syndrome (ARDS) diagnoses for compliance with international definitions [23–25].

Secondary outcomes

The following secondary outcomes were recorded: all-cause mortality at day 90; acute respiratory distress syndrome by day 28 (PaO_2/FiO_2<200 mmHg [26]); durations of mechanical ventilation, ICU hospitalization, and hospital stay.

Blood sample collection

Three samples were collected in the IBIS and the PREV-HAP cohort. In the IBIS cohort, the first was collected upon ICU (maximal first 48 hours, called day 0), the subsequent were harvested at day 3-4, and at day 6-7. In the PREV-HAP cohort, the first sample was collected upon randomisation before any treatment (maximal first 48 hours of ICU admission, called day 0), the subsequent samples were harvested at day 3 (immediately before the second injection of IFN-γ or placebo), and at day 7. Blood was collected into EDTA-tubes, centrifuged at +4°c, separated into plasma and frozen immediately at – 80°C before centralized metabolomic analysis.

Metabolomic measurement

1For extraction, plasma samples were thawed on ice for 30-60 min before 1/10-dilution into aq. 80% LCMS-grade methanol for protein precipitation and elimination by centrifugation at room temperature (14.000g for 15 min). Pellet supernatant was analysed by untargeted Liquid chromatography/mass spectrometry by General Metabolomics (Cambridge, MA). For each cohort, samples were run in random order, and each sample was injected twice. Loss of signal throughout the run, which is classical for large cohort acquisition, was corrected by Total Ion Count (TIC) normalization method, in which each metabolite in a sample is divided by the total number of ions observed in the sample [27] Metabolite putative annotations were generated based on compounds in the Human Metabolome Database, KEGG, and ChEBI databases using accurate mass per charge (tolerance 0.001 m/z) and isotopic correlation patterns (Table E1 in the online data supplement for correspondence between human-readable annotation and scientific names).

Linear regressions on metabolome data

Metabolome data has been normalized using a log10 transformation tolerating negative values. With the R package limma (version 3.56.2), linear regressions were performed for each metabolite. The design included the HAP status as the primary predictor and clinical covariates (sex, age, durations of ICU stay and mechanical ventilation, Glasgow, SOFA and SAPSII scores, number of comorbidities and the timepoints).

Metabolites correlations and enrichment analysis

The Spearman correlation coefficients were calculated with the package psych (version 2.4.1), between the significant metabolites (adjusted p-value of the previous linear regressions < 0.05). P-values were adjusted with false discovery rate (Benjamini-Hochberg (BH) method). Using the *hclust* function (stats package, version 4.3.2), we identified a cluster of 88 metabolites that included most of the core metabolites and their most strongly correlated counterparts. This correlation-based clustering allowed us to capture a broader metabolic signature potentially linked to shared biological processes. We then performed an over-representation analysis using the *MetaboAnalystR* package (version 4.0.0), leveraging the list of 88 metabolites. These were mapped to the Human Metabolome Database (HMDB) to identify enriched metabolic pathways.

Unsupervised longitudinal consensus clustering

The metabolites differentially abundant between HAP and no HAP patients were selected for the longitudinal consensus clustering of the discovery cohort. Every patient with complete data (D0, D4 and D7 samples, n=82) has been assigned to a cluster using the R package longmixr (version 1.1.0). The cohort was separated into 2, 3 or 4 clusters based on 50 runs of subsampling (80 % of the patients) and clustering. The clinical covariates included in the linear regression models were also

used in the longitudinal consensus clustering. The optimal number of clusters was identified with the consensus cumulative distribution function (CDF) plot, in which the flattest curve indicates higher consensus.

Statistical comparison of the clusters

The clusters of patients have been compared using Fisher's exact tests and Wilcoxon rank-sum tests for the categorical and continuous variables, respectively. The durations of ICU stay and mechanical ventilation were compared with Cox proportional hazards regression models (survival package, version 3.5-7). The competing risk of death was addressed by censoring data of patients who died in ICU. The metabolites' abundances were compared between clusters with pairwise Mann-Whitney Wilcoxon tests at each timepoints and the resulting p-values were adjusted with BH method. The list of metabolites significantly different between the Moderate or High risk vs Low risk patients at D4 and those different between Low or Moderate risk vs High risk patients at D7 have been associated with metabolic pathways using *MetaboAnalystR* as previously detailed.

Validation of the clusters using an external cohort

Using the scaled and centered abundance of the significant metabolites and the cluster labels, decision trees have been trained with the package FFTrees (version 2.0.0.9006). A first tree was trained to classify patients into the Moderate risk group with the D0 metabolite abundance. A second tree was trained to classify the remaining patients (Low and High risk groups) using D4 metabolites abundances. Both trees were applied to the scaled and centered metabolites abundance of the validation cohort. The patients who were not classified in the Moderate risk group with the first decision tree (probability threshold < 0.5) were classified as either Low risk or High risk group using the second tree (probability threshold ≥ 0.5 and < 0.5, respectively). We also built a classification decision tree using the D0 and D4 abundance of the same metabolites with the package rpart (version 4.1.21) to identify the best classification scheme.

Principal Component Analysis (PCA)

For each timepoint, a PCA has been performed using the package mixOmics (version 6.24.0). The PCA of the IBIS cohort was based on the whole metabolome dataset (n=1295 metabolites), while the PCA of the PREV-HAP cohort was based on the metabolites significantly different between HAP and no HAP patients (n=19 metabolites).

Generation of epigenetic and transcriptomic data in circulating monocytes

Monocytes were isolated from PBMCs with the EasySep human monocyte enrichment kit without CD16 depletion (Stemcell Technologies), frozen and stored at -80 °C till analysis. Assay for transposase-accessible chromatin with sequencing (ATAC-seq) experiment was performed as previously described [28] . Briefly 5 x 10^4 monocytes were centrifuged at 500 x g for 5 min at 4°C and incubated a transposase reaction mix containing 2 µl Tagment DNA Enzyme (Illumina), 12.5 µl 2x Tagment DNA Buffer (Illumina), 0.25 µl 1% digitonin (Promega) and 10.25 µl nuclease free water for 30 minutes at 37 °C. DNA was purified with the MinElute kit (Qiagen) following manufacturer's instructions.

Chromatin immunoprecipitation (CHIP) for H3K18 lactylation

Library preparation, sequencing and processing have been performed as previously reported in detail [29]. Briefly, 1.5 x10^6 monocytes were fixed in 1% methanol-free formaldehyde and quenched with glycine. Cells were lysed in lysis buffer (1% SDS; protease inhibitor cocktail (Roche); 20 mM HEPES (pH 7.6)) and sonicated (S220 focused-ultrasonicator; Covaris). Samples were incubated overnight with antibodies against H3K18la (rabbit pAb, PTM-1406, PTM Bio), H3K27ac (pAb-196-050, Diagenode), and immunoprecipitated using Dynabeads Protein A/G (Thermo Fisher Scientific). DNA was purified with Qiaquick MinElute PCR purification Kit (Qiagen) following manufacturer's instructions. ChIP-seq libraries were prepared using the KAPA HyperPrep Kit according to manufacturer's protocol and as previously described in detail [29]. Libraries were paired-end sequenced to a read length of 50 bp on an Illumina NextSeq500 or Nextseq2000.

Epigenetic comparisons of the clusters in the validation cohort

A table of unnormalized counts per peak were generated from ATAC-sequencing and H3K18 lactylation ChIP-sequencing data. Each ATAC and H3K18la peak was annotated to the nearest gene (within 1,000 kbp) using GREAT (Genomic Regions Enrichment of Annotations Tool), with the human genome GRCh37 (hg19) as reference (PMID: 20436461). Genomic sites separated by less than 12.5 kbp were combined into super-enhancers and their unnormalized counts summed. Therefore, one super-enhancer could be associated to several genes. Normalization and pairwise comparisons of the three clusters of patients (low, moderate and high risks) were performed using the function DESeq of the R package DESeq2 (version 1.42.1) with the alpha parameter of independent filtering set to 0.2. The significance

threshold was set to 0.05. The relation between the lactylation of the super-enhancer 1508 and the expression of S100A9, S100A8 and S100A12 genes has been studied with linear regression based on their variance-stabilising-transformed counts.

Numeric twin data

Synthetic data were generated using a patient-centric method called avatar [2]. Developed for sensitive biomedical data, the method is patient centric as it uses a local model to generate random new synthetic data, called « avatar data », for each sensitive individual. We used it to generate synthetic cohorts with different abundance for each cluster of patients and improve statistical power by oversampling. Each synthetic dataset was generated using the following process. The original data from the metabolome and clinical were split by patient cluster (3 clusters). We then created 3 synthetic data pools, one for each cluster, by applying the avatar method multiple times on each cluster. Finally, we sampled the pools to create the synthetic dataset with a specific abundance of each cluster. For each cluster of patients, we generated a dataset with 50%, 70%, and 90% abundance, the remaining was equally shared between the two other clusters. In total, we produced 9 synthetic data based on metabolome best features and 9 based on clinical data.

Comparing the effect of interferon gamma on real and simulated data

The relative risk of interferon gamma on the rates of HAP, ARDS, serious adverse events and mortality was calculated with the package DescTools (version 0.99.5), and hazard ratio (HR) for the durations of ICU stay and mechanical ventilation were determined with Cox proportional hazards regression models. These metrics were calculated for each cluster of patients identified in the validation cohort and each synthetic dataset generated with the numeric twin method. Forest plots were created with the package forestplot (version 3.1.3). The number of adverse events in the real data of treatment groups was compared with Mann-Whitney-Wilcoxon tests for each cluster. Simulated datasets with varying cluster proportions were also generated by random sampling (with replacement) of PREV-HAP patients after their classification. All simulated datasets contained 74 patients (70% of the cohort size) and had a varying proportion of high risk and low risk patients. Each kind of dataset has been simulated 50 times. After every simulation, the treatment response was evaluated using the duration of ICU stay in Cox proportional hazard regression models. A HR >1 indicates a shorter ICU stay in treated patients compared to placebo. Therefore, with a HR >1 or <1, the treatment was considered beneficial or harmful for the corresponding simulation, respectively. For p-values >0.05, the treatment was considered neutral for the given simulation.

Additional details on the method for blood metabolome quantification, epigenetic analyses and PBMC isolation are provided in an online data supplement.

Results

Discovery cohort, sampling protocols and experimental approaches

Based on sample availability in the IBIS cohort, we selected 330 blood samples upon ICU admission, and on days 3-4 and 6-7 following admission of 128 severe brain-injured patients. Baseline characteristics and clinical outcomes are described in Table 1**.** Of the 128 patients analysed, 57 (45%) had developed HAP and 21 (16%) HAP-induced ARDS. All HAP developed before day 10 of hospitalisation. Plasma samples were analysed by flow-injection mass-spectrometry for metabolomic profiling, and 518 different metabolites were identified and annotated.

Metabolite core associated with HAP in the discovery cohort.

Principal Component Analysis (PCA) revealed emerging differences in the metabolomic profiles of patients who developed HAP or HAP-induced ARDS compared to those who did not, mostly at day 6-7 of ICU stay (PCA, Figure 1A). We identified the metabolites associated with HAP using linear regressions adjusted with several clinical covariates. By setting the False Discovery Rate (FDR)-adjusted p-value threshold to 0.05, we identified a panel of 21 metabolites with differing abundances in samples from patients with or without HAP (Figure 1B). We excluded propofol, which is a hypnotic drug whose doses are increased in patients with HAP and ARDS and its derivative 4-hydroxypropofol. Among the 19 remaining metabolites, 13 were significantly correlated with each other (Figure E1 in the online data supplement) and were involved in the fatty acid biosynthesis pathway (Figure 1C).

Using Longmixr, an unsupervised longitudinal consensus clustering tailored to incorporate categorical (sex) and continuous data (age, metabolite abundances) [30], we identified three metabolic response patterns which were associated with HAP and ARDS (Figs 1D-E and Fig E2 for optimal cluster number definition). We thus labelled them as low-risk, moderate-risk and high-risk metabolic response patterns. The clinical characteristics and outcomes of patient based on their metabolic response patterns are reported in Table E2, and the time-to-successful weaning from mechanical ventilation is shown in Figure 1F**.** Then, we identified the lists of metabolites with different abundance levels between patterns and found that fatty acid biosynthesis and β-oxidation of very long-chain

Table 1 Population characteristics

	Discovery cohort (observational - IBIS)			Validation cohort (randomized PREV-HAP)		
	Total	**No HAP**	**HAP**	**Total**	**Placebo**	**Interferon gamma 1b**
Number of patients, *n*	128	71	57	105	51	54
Age, *years,* median (IQR)	43.6 (26.9-58.1)	44.6 (27.7-56.0)	41.1 (25.0-58.1)	57.6 (41.6-65.7)	57.6 (42.7-66.2)	57.0 (41.6-64.7)
Male, *n (%)*	98 (77)	48 (68)	50 (88)	68 (65)	35 (69)	33 (61)
Pathology, *n (%)*						
Stroke	13 (10)	6 (8)	7 (12)	NA	NA	NA
Other pathology	1 (1)	0 (0)	1 (1)	NA	NA	NA
Trauma	114 (89)	65 (92)	49 (86)	50 (48)	23 (45)	27 (50)
Medical/surgical septic	NA	NA	NA	6 (6)	4 (8)	2 (4)
Medical/surgical non septic	NA	NA	NA	49 (47)	24 (47)	25 (46)
Steroids, *n (%)*	NA	NA	NA			
Dexamethasone				1 (1)	1 (2)	0 (0)
Hydrocortisone				28 (27)	11 (22)	17 (31)
No steroids				78 (74)	39 (76)	37 (69)
Comorbidities,*n* (%)						
Cardiac insufficiency (NYHA >2, Marked limitation of physical activity)	1 (1)	1 (1)	0 (0)	4 (4)	3 (6)	1 (2)
Chronic kidney failure (MDRD GFR < 50 mL/min)	3 (2)	2 (3)	1 (2)	0 (0)	0 (0)	0 (0)
Neurological history	18 (14)	13 (18)	5 (9)	14 (13)	9 (18)	5 (9)
Chronic obstructive pulmonary disease	2 (2)	0 (0)	2 (4)	3 (3)	2 (4)	1 (2)
Active smoking	34 (27)	16 (23)	18 (32)	34 (32)	19 (37)	15 (28)
Diabetes mellitus	9 (7)	5 (7)	4 (7)	10 (10)	5 (10)	5 (9)
Cancer within 5 last years	3 (2)	2 (3)	1 (2)	4 (4)	3 (6)	1 (2)
SOFA, median (IQR)	8.5 (6.0-11.0)	9 (7-11)	8 (6-10)	7 (5-9)	6 (5-9)	7.5 (5-9.8)
SAPS-II, median (IQR)	43.0 (34.0-54.3)	44.0 (35.5-55.5)	42 (31-51)	45 (37-52)	44.0 (36.0-51.5)	45.0 (37.3-53.5)
Blood count at admission, *G/L*						
Total leucocytes	15.5 (12.3-18.8)	15.7 (13.1-19.3)	14.7 (12.1-17.8)	11.8 (9.6-15.6)	12.9 (10.3-15.5)	11.3 (9.3-15.5)
Lymphocytes	0.9 (0.4-1.6)	0.9 (0.4-1.6)	0.9 (0.4-1.6)	0.9 (0.6-1.2)	0.8 (0.6-1.1)	0.9 (0.6-1.2)
Monocytes	0.9 (0.3-1.3)	0.8 (0.2-1.3)	0.9 (0.5-1.2)	0.8 (0.5-1.1)	0.8 (0.5-1.1)	0.7 (0.5-1.1)
Neutrophils	10.9 (5.5-15.5)	11.3 (6.0-15.8)	10.5 (5.4-14.8)	8.8 (6.5-12.0)	9.1 (7.0-12.0)	8.7 (6.1-12.0)
Tracheobronchitis, n(%)	8 (6)	8 (11)	0 (0)	23 (22)	18 (35)	5 (9)
Bacterial HAP, n (%)	57 (45)	0 (0)	57 (100)	27 (26)	8 (16)	19 (35)
Early HAP, n (%)	29 (51)	0 (0)	29 (51)	13 (48)	4 (50)	9 (47)
Late HAP, n (%)	28 (49)	0 (0)	28 (49)	14 (52)	4 (50)	10 (53)
Acute respiratory distress syndrome, *n (%)*	21 (16)	0 (0)	21 (37)	7 (7)	1 (2)	6 (11)
Mechanical ventilation duration, days*	11.0 (6.8-24.0)	7.0 (4.5-11.5)	23 (13-32)	13 (8-23)	15 (8-22)	12.5 (8.0-22.5)
ICU length of stay, days*	18.0 (10.0-33.3)	10 (7-19)	31 (20-41)	18 (12-29)	18.0 (10.5-28.5)	17.5 (13.0-29.3)
In ICU death	32 (25)	20 (28)	12 (21)	26 (25)	13 (25)	13 (24)
All-cause mortality day 90, n (%)	36 (28)	21 (30)	15 (26)	28 (27)	15 (29)	13 (24)

ICU: Intensive Care Unit, HAP; hospital-acquired pneumonia, MDRD GFR: Modification of diet in renal disease glomerular filtration rate, NYHA: New York Heart Association, SAPS-II: Simplified Acute Physiology Score II, SOFA: sequential organ failure assessment

fatty acids pathways were increased in the high-risk metabolic response versus other responses at day 6-7, the latter being also increased in the moderate and high-risk at day 3-4 (Figures 1G-H). This series of analyses demonstrated an association between HAP and the time course of fatty acid metabolism alterations in ICU patients.

Development of a simplified metabolomic score individually associated with HAP severity.

These endotypes were derived from the longitudinal modelling of multiple metabolites, which limits their applicability for patient classification and does not enable an external validation in an independent cohort.

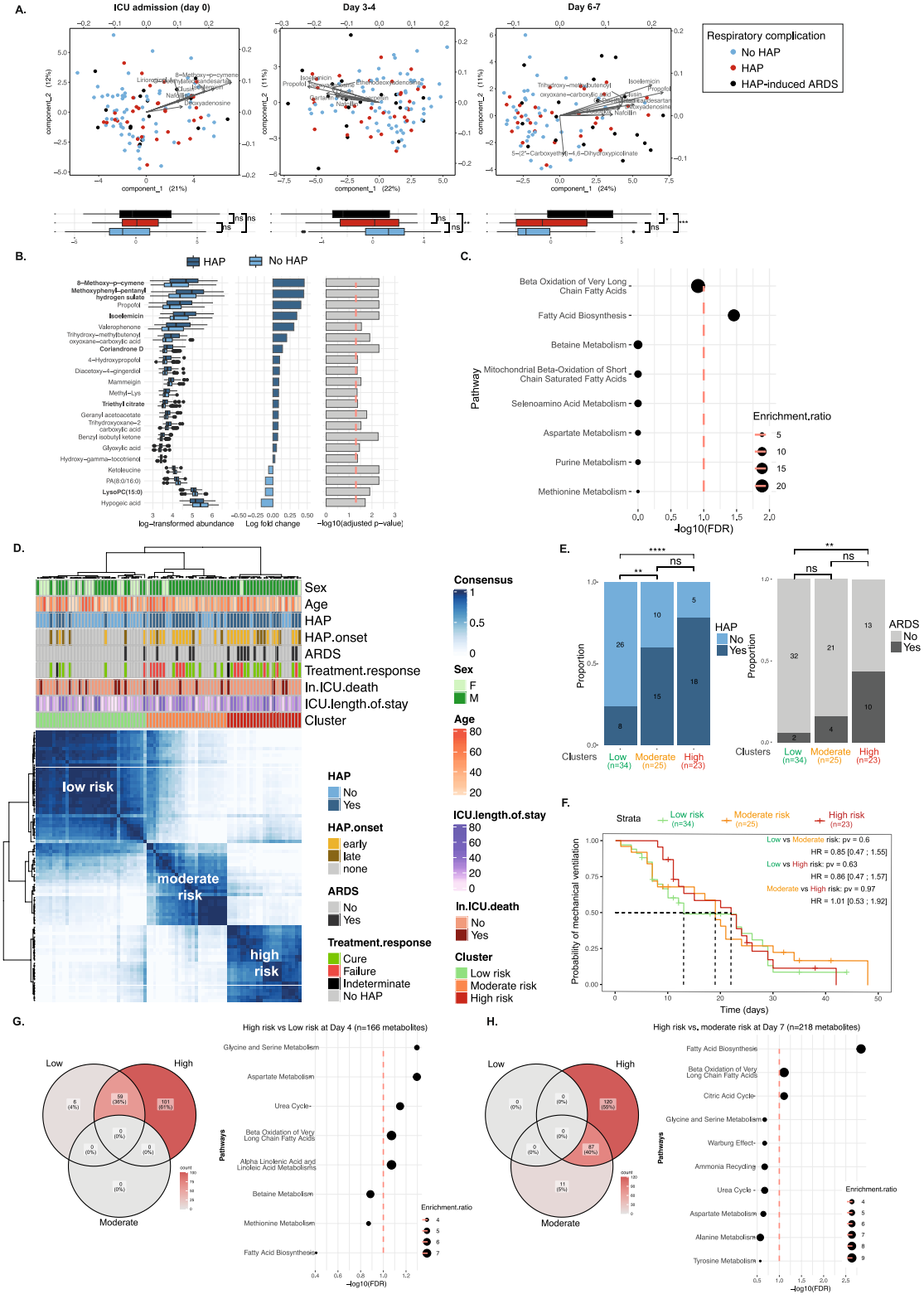

Fig. 1 (See legend on next page.)

(See figure on previous page.)

Fig. 1 Metabolomic response to critical illness is associated with respiratory complications in critically ill patients. **A**. PCA representations of plasma metabolome at day 0, day 3-4 and day 6-7 after ICU admissions in patients who remained uninfected or developed HAP, or HAP-induced ARDS. The PC1 values were compared between clusters using Mann-Whitney Wilcoxon tests. **B**. The log-transformed quantification of the 21 metabolites differentially abundant between HAP patients and no HAP patients (left), the log fold change values (middle) and the corresponding adjusted p-values (right). The orange line represents the threshold of significance (adj. pv < 0.05). **C**. Metabolic pathways represented by the 13 metabolites-core and their related metabolites (n=88 metabolites). The vertical line corresponds to the significance threshold set to 0.1 using adjusted p-value. **D**. The consensus matrix reflects the similarity between each pair of patients. A high consensus indicates a high similarity between the two patients considered. **E**. Proportion and number of patients with HAP and ARDS among the three clusters identified. **F**. Probability of being mechanically ventilated across time for each cluster. HR = hazard ratio. **G-H**. Metabolic pathways increased in moderate- and high-risk metabolic response at day 4 and in high-risk at day 7. The vertical line corresponds to the significance threshold set to 0.1 using adjusted p-value

Therefore, we employed a stacked machine learning model consisting of spectral clustering and Fast and Frugal Trees (FFT) to define a parsimonious classification scheme using a minimal number of metabolites. FFT-based modelling offered a simple, 4-factor decision tree that individually classified samples as low, moderate or high-risk metabolic response based on the abundance of Triethyl citrate and methoxyphenyl pentanyl hydrogen sulfate at day 0, and 8-methoxy-p-cymene, Isoelemicin and methoxyphenyl pentanyl hydrogen sulfate at day 3-4 (Figure 2A**)**. This FFT-based classification of the metabolic response remained reasonably associated with HAP and ARDS with accuracies of 0.661 (95%CI 0.650-0.677) and 0.716 (95%CI 0.676-0.736), respectively (Figures 2B-D). We also tested a score built by a Classification Decision Tree, which can improve the model's accuracy and interpretability, but usually uses more variables than FFT. The Classification Decision Tree-based model included 3 factors but did not have significantly better accuracy than the FFT-based score (FigureE3).

Validation of the simplified metabolome signature in an independent patient cohort.

We tested the robustness of the FFT classification scheme in an independent, multicenter cohort of critically ill patients suffering from diverse medical conditions. We analysed 315 blood samples collected on days 0, 3 (immediately before the second injection of the study treatment), and 7 (immediately before the fourth injection of the study treatment) after the inclusion in multicentre, placebo-controlled randomised clinical trials evaluating interferon-gamma (IFN-γ) treatment for the prevention of HAP in 105 critically ill patients (Figure 2E and Table 1 for study population characteristics) [10]. First, we questioned whether IFN-γ treatment could bias the metabolite-based classification. We validated differences in metabolomic architectures between groups (Figure 2F and Table E1 for clinical characteristics) and found no statistically significant differences in day 3 blood levels of the 19 metabolites used to define the unsupervised clusters between the placebo and the supplement (Supplementary Figure E4). Moreover, the percentages of patients classified as low, moderate, or high risk did not differ between the discovery IBIS cohort and the placebo and interferon PREV-HAP cohorts (Supplementary Figure E5). This series of analyses suggests that IFN-γ treatment was not associated with the risk of being assigned to a specific cluster. Finally, we observed similar temporal patterns of the 4 metabolites used for the FFT classification among the discovery and validation cohorts (Fig 2G**),** and we confirmed that HAP and ARDS rates were higher in patients with metabolic response classified as moderate or high risk than those considered low risk (Fig 2H), thus confirming the robustness of the association between the metabolic response patterns and HAP.

Plausible biological mechanisms supporting the association of metabolome heterogeneity with immune profile

A vital step in establishing the relevance of high-throughput machine learning clusterisation results is the identification of plausible pathophysiological mechanisms that support causality. We have previously reported an association between early epigenetic regulation of circulating monocytes, interferon pathway activation and severe respiratory complications in critically ill patients [6]. We thus asked if the metabolome-based endotypes were associated with monocyte epigenetic profiles. Based on sample availability, we accessed monocytes from 15 patients from the PREV-HAP collected at day 0 (upon ICU admission and before study intervention injection) and studied two layers of epigenetic regulation: ATAC-sequencing which provides information of DNA accessibility to transcription factor and transcriptional machinery and histone lactylation (H3K18la), a lactate-related histone modification regulated by metabolic activity and associated with gene expression [29, 31]. Using ATAC-seq, we identified 6 and 2 super-enhancers with different accessibility levels between moderate and low-risk metabolic patterns and between high and low-risk patterns, but no difference in active regions between high-risk and moderate-risk groups at day 0 (Figure 3A). However, we identified 2 super-enhancer regions with H3K18la peaks that were significantly increased in high-risk patients at day 0 compared to moderate-risk patients (Figure 3B). The 1508th super-enhancer, located on chromosome 1, was the most differentially lactylated in high-risk metabolic response. The annotation revealed

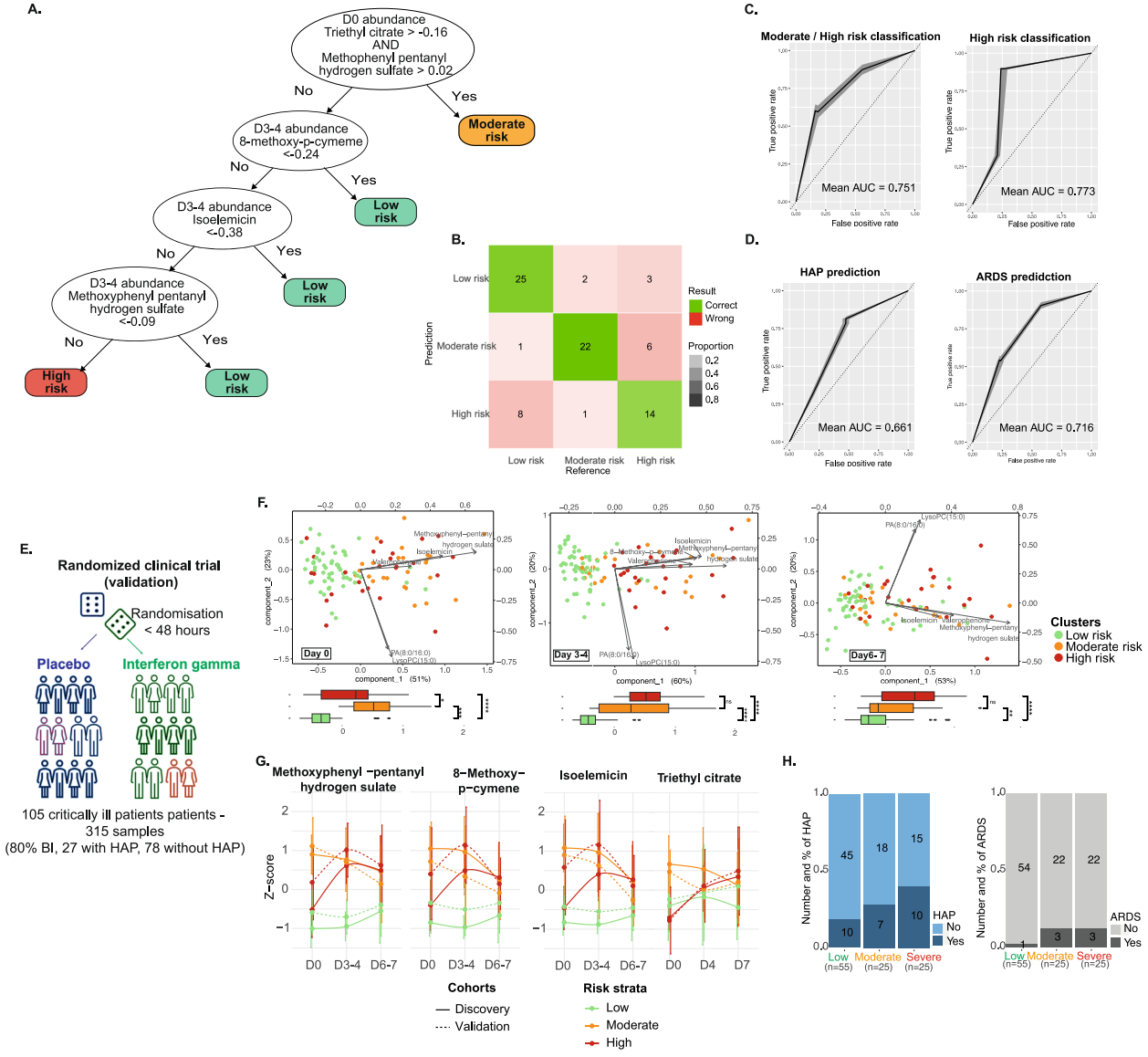

Fig. 2 Development and validation of a metabolite signature associated with respiratory complications in critically ill patients. **A**. Fast-and-frugal tree-based staging scheme to classify patients as low, moderate and high risk of respiratory complications. **B**. Confusion matrix for FFT-based score classification into low, moderate and high risk in the discovery IBIS cohort. **C**. Receiver operating characteristic (ROC) curve of moderate/high-risk (left) and high-risk (right) cluster classification applying a 10-fold cross-validation scheme. The model evaluation displays the cross-validation error as a (ROC) curve, with a 95% confidence interval shaded in grey. **D**. ROC of HAP and ARDS applying a 10-fold cross-validation scheme. The model evaluation displays the cross-validation error as a receiver operating characteristic (ROC) curve, with a 95% confidence interval shaded in grey. **E**. External cohort of 105 critically ill patients randomised to interferon-gamma or placebo treatments, with samples available for blood metabolomic analysis at D0, D4 and D7 of ICU stay. **F**. PCA representations of plasma metabolome at day 0, day 4 and day 7 after ICU admissions in low, moderate or high-risk patients. The PC1 values were compared between clusters using Mann-Whitney Wilcoxon tests. **G**. Variations of the standardized metabolites levels included in FFT-based staging scheme. The colours indicate the clusters (low, moderate and high-risk) and the line type indicates the cohort (discovery or external validation). **H**. Numbers and frequencies of HAP and ARDS in risk strata defined by FFT-based staging scheme in the entire population (pooling placebo and interferon-gamma groups)

that it was associated with 4 genes of the S100 family (*S100A7A*, *S100A9*, *S100A8* and *S100A12*) and with *PGLYRP4* (Peptidoglycan Recognition Protein 4). While this super-enhancer was more lactylated at day 0 in all critically ill patients compared to healthy donors, it was less lactylated in moderate-risk patients than in the two other clusters (Figure 3C). We observed a positive correlation between the level of super-enhancer lactylation and the mRNA levels of S100A8, S100A9, and S100A12, indicating direct epigenetic regulation of these gene transcripts (Figure 3D). Taken together, these exploratory results suggest an association between endotypes defined

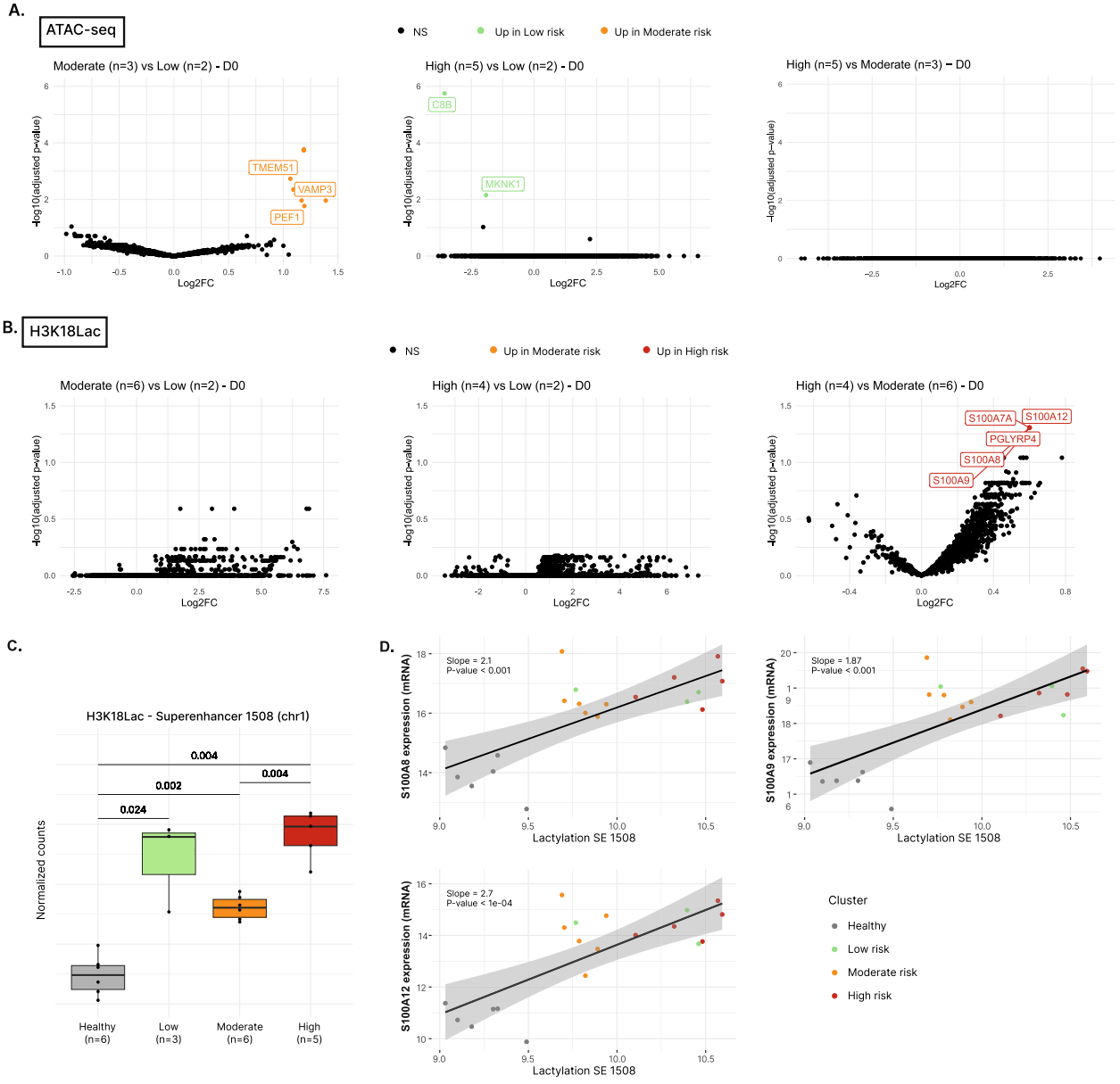

Fig. 3 Monocyte epigenetic signatures differ across patient risk levels at ICU admission. **A**. Pairwise comparisons of the chromatin accessibility (ATAC-seq) and (**B**) H3K18 lactylation marks at the super-enhancer level at day 0, between low-, moderate- and high-risk patients. Each dot represents a super-enhancer, in which the peaks distant by less than 12.5 kbp have been combined. Therefore, a dot can be associated to several genes. **C**. Normalized counts of H3K18la marks in the 1508th super-enhancer at day 0 in each risk strata and healthy donors. **D**. Linear relations between H3K18la marks of the 1508th super-enhancers and the gene expression of S100A8, S100A9 and S100A12 at day 0

by plasma metabolite levels and metabolism-dependent epigenetic regulation in monocytes at Day 0, but mechanistic studies remain necessary to support definitive conclusions.

Simplified metabolome signature for the identification of responders and non-responders to interferon-gamma treatment

Another crucial step in validating the clinical relevance of metabolic response patterns is to assess whether they are associated with treatment outcomes. Simply identifying a signature associated with HAP does not inherently ensure its utility for personalizing treatment. IFN-γ treatment restored the glycolytic/oxidative balance of exhausted lymphocytes in septic patients [18], and most of the metabolites used for patient classification were involved in fatty acid biosynthesis and oxidation. Thus, we leveraged access to biological samples collected during the PREV-HAP trial to test the hypothesis that

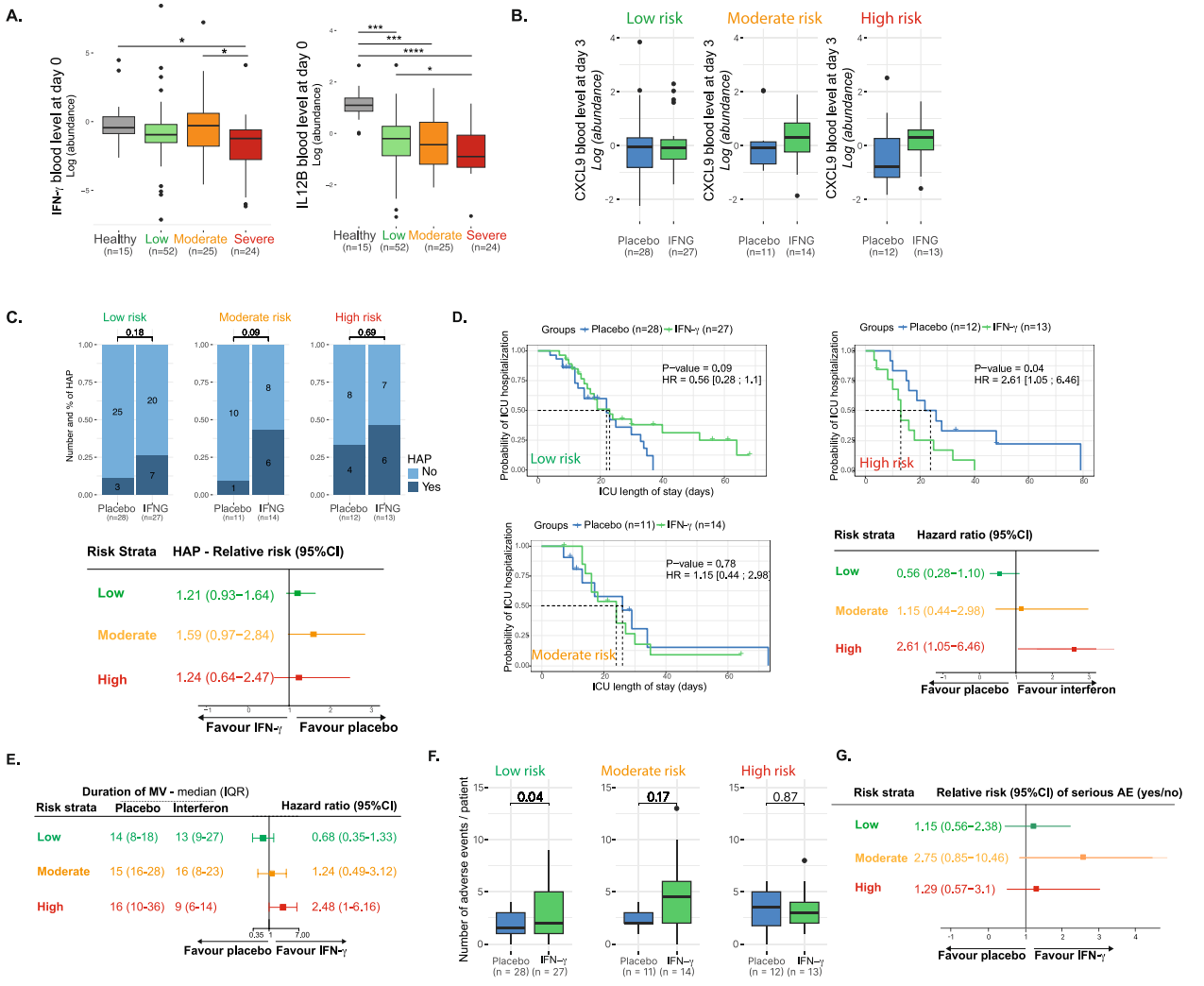

Fig. 4 Metabolite-based risk classification is associated with the response to interferon gamma treatment. **A**. Interferon-gamma (IFN-γ) and IL12B blood levels on day 0 in healthy controls and risk strata. **B**. CXCL9 blood levels on day 3 in patients treated with placebo or interferon gamma, stratified by the risk strata. **C**. Numbers and frequencies of HAP in risk strata defined by FFT-based staging scheme in the placebo and interferon-gamma groups, and relative risk for HAP in risk strata. **D**. Kaplan-Meier curves for the probability of ICU hospitalisation with placebo and interferon-gamma treatment in low, moderate and high-risk strata, and the associated hazard ratio for ICU discharge with interferon gamma 1b treatment in risk strata. Hazard ratio (> 1) indicates a higher chance of ICU discharge with interferon gamma treatment. **E**. Hazard ratio for weaning from invasive mechanical ventilation with interferon gamma 1b treatment in risk strata. Hazard ratio (> 1) indicates a higher chance of weaning from mechanical ventilation with interferon gamma treatment. **F**. Number of adverse events between treatment groups in each risk stratum. **G**. Relative risk of having at least one serious adverse event with IFN-γ treatment in risk strata. Relative risk (> 1) indicates a higher risk of serious adverse event with treatment

the effects of IFN-γ treatment varied with metabolic response patterns.

We observed that the blood concentrations of IFN-γ and interleukin 12B (IL-12B, which is produced by myeloid cells and induces the production of IFN-γ by lymphocytes) at day 0 were lower in patients with a high-risk metabolomic signature compared to those with a low-risk metabolomic signature or healthy controls (Figure 4A). Moreover, IFN-γ treatment increased the blood concentration of CXCL9, an interferon-stimulated chemokine, in high-risk patients but not in low-risk patients (Figure 4B), suggesting that the immune response to IFN-γ treatment varied with the metabolic patterns.

Supporting this hypothesis, we found that IFN-γ treatment tended to increase the risk of HAP in patients with low/moderate-risk metabolic responses but not in those with high-risk metabolic responses (Figure 4C). However, these results can be biased by IFN-γ effects on body temperature and leukocyte counts, which can increase false-positive HAP diagnoses. Thus, we studied the treatment effect on the duration of mechanical ventilation and ICU length of stay, which are relevant patient-related outcomes and are frequently used as a proxy for HAP severity [32]. IFN-γ treatment decreased the probabilities of being discharged alive from the ICU and of being successfully weaned from mechanical ventilation in patients

with low-risk metabolic response, but the intervention increased these probabilities in patients with high-risk metabolic response (Figures 4D-E)**.** IFN-γ had no effect on the time to mechanical ventilation or ICU discharge in patients with moderate-risk metabolic response. **Figure E6** shows the relative risk of day-28 all-cause mortality for IFN-γ across patient strata. Patients with low-risk metabolic response had more adverse events (AEs) when treated with IFN-γ compared to placebo (Figure 4F**).** In contrast, the treatment did not increase harm in patients with high-risk metabolic responses. The relative risk of developing severe AEs with IFN-γ treatment was increased in patients with moderate-risk metabolic response patterns (Figure 4G). This series of results demonstrated that metabolic response classification based on a 4-metabolite signature enabled the identification of responders and non-responders to IFN-γ treatment.

Exploratory subgroup analyses

Given the temporal overlap between metabolite-level measurements (up to day 4) and early HAP onset (days 2–4), we evaluated the accuracy of the metabolic score in predicting late HAP (> or = day 5 after hospitalisation). Our analysis revealed that the proportion of late HAP cases was significantly higher among high-risk patients than among low-risk patients in both the discovery (IBIS) and validation (PREV-HAP) cohorts (Figure E7). This a posteriori analysis suggests that these endotypes are a predisposition to unfavourable respiratory outcomes rather than a signature of active, early-stage infection.

To test the generalizability of our findings, we performed a post hoc subgroup analysis comparing predictive accuracy between trauma and non-trauma patients. We found that the temporal patterns of the 4 metabolites used to calculate the risk-classification score were similar between trauma and non-trauma patients in the PREV-HAP cohort (Figure E8A). Moreover, the accuracy of HAP prediction in non-trauma patients did not differ significantly from that in the total population (AUCs of 0.61 and 0.60, respectively; Figure E8B).

Simulation of population enrichment in IFN-γ on the estimation of interferon gamma-1b effects

Finally, in exploratory analyses, we investigated the effects of varying the proportions of patients with low- and high-risk metabolic responses on the probability of concluding benefit, harm, or no effect in simulated randomised trials testing IFN-γ. Thus, we generated synthetic data from the validation cohort to address class imbalance. The predicted treatment effect ranged from an 80% chance of benefit (for a 75% high-risk population) to an almost 25% chance of harm (for a 75% low-risk population; Figure E9A-B).

Discussion

In the present study, we report a longitudinal exploration and comprehensive analysis of blood metabolome alterations in critically ill humans. We identified inter-individual heterogeneity in the metabolite response patterns. The development and external validation of a simplified metabolic pattern signature enable prediction of HAP and ARDS and identification of responders and non-responders to IFN-γ therapy after a single treatment injection.

A decreased interferon-gamma production was associated with critical illness severity and unfavourable outcomes [33, 34]. Thus, IFN-γ treatment has been proposed to prevent and treat difficult-to-treat infections [35]. However, in a randomised clinical trial we reported that the administration of IFN-γ in an unselected population of critically ill patients was associated with HAP and ARDS development [10], suggesting that the defect in IFN-γ production is an adaptive response to critical illness in the majority of patients and should be considered as a severity marker rather than a causal mechanism. Aligning with this hypothesis, we described that the epigenetic inhibition of IFN-γ production by myeloid cells was associated with reduced risk of HAP in severe brain-injured patients [6]. However, we and others identified responders to IFN-γ [36–38], suggesting that low IFN-γ production is a cause of mortality in a subgroup of patients characterised as immune-paralysed. Significantly, the ability to early discontinue IFN-γ treatment in non-responders could reduce the risk of adverse events and enable testing other immune therapies in non-responders who constituted the largest fraction of the cohort.

We identified a core metabolite response to critical illnesses associated with HAP, involved in the β-oxidation of very long-chain fatty acids and fatty acid biosynthesis. These two functions support cell proliferation and survival in nutrient-poor conditions. Very long-chain fatty acids are essential constituents of cellular lipids, such as sphingolipids and glycerophospholipids, and can serve as precursors of lipid mediators. Fatty acid oxidation becomes a vital energy source in case of acute inflammation, such as during sepsis [39]. Several amino acid metabolisms were identified in the metabolic response to HAP at day 3-4, suggesting that the increased proteolysis participates in the cellular energy sourcing and aligns with the liver's increased use of amino acids to sustain the acute inflammation phase. Our study suggests that approaching metabolite endotypes at the bedside can help understand the inter-individual heterogeneity in the response to metabolite-targeting treatments.

Histone lactylation is a recently identified epigenetic modification associated with lactate-mediated regulation of gene expression, highlighting the connection

between intracellular glycolytic metabolism and chromatin dynamics [31]. According to the metabolome-based clusters, we could identify differential levels of histone lactylation at a superenhancer associated with the regulation of S100 family genes in circulating monocytes of patients. More precisely, patients classified in the high-risk group, with the highest proportion of severe HAP and lower blood levels of IFNG and IL12B, exhibited the highest levels of histone lactylation. These results suggest an association between plasma metabolome and intra-monocyte metabolome heterogeneity. However, the small sample size of these epigenetic analyses limits the robustness of this association. Further validation is necessary before a definitive link can be established between the early epigenetic regulation of monocytes and the circulating metabolome.

Significant effort has been made over the past few decades to define baseline biomarkers useful for personalizing treatment, yet these have seen limited translation into clinical practice. Our results suggest the longitudinal monitoring of metabolic profiles represents a promising approach in the context of personalized immunotherapy. The next step should be translating our high-throughput metabolic signature into a simple, easily measurable set of metabolites. For example, given their association with fatty acid metabolism, comparing lipid compositions between these endotypes could facilitate their identification at the bedside [40] .

Our study has several limitations. Firstly, given the observational nature of our data, we cannot conclude whether metabolome alterations contribute to respiratory complications or if they are their consequences. Thirdly, our study samples were collected early, in all cases during the first week of hospitalization, and the signature accuracies could decrease with time. Fourthly, the score development was conducted in a homogeneous population of severely brain-injured patients, primarily trauma cases, from only two centers. This may limit the generalizability of the current findings to other ICU populations. Although the validation dataset included samples from a heterogeneous group of critically ill patients with one or more acute organ failures across nine French ICUs, and a posteriori subgroup analysis of non-trauma patients reproduced the same findings, extrapolating our findings to non-trauma patients should be done cautiously. Finally, some metabolites used for clustering were measured after randomization in the validation cohort, possibly introducing causal ambiguity. Indeed, the cluster assignment itself may be influenced by IFN-γ treatment in the PREV-HAP cohort.

Conclusion

This study revealed an association between the time course of fatty acid metabolism and HAP, thereby advancing our understanding of HAP pathophysiology. Early identification of metabolic response patterns is feasible from days 3 to 4 using a simplified 4-metabolite score. While this score cannot be used to predict early HAP, it remains useful for identifying patients at high risk of late HAP, those likely to respond favourably if IFN-γ treatment is prolonged for 10 days, and those at low risk who may exhibit an unfavourable response to treatment. Theoretically, this metabolic classification could enable the early discontinuation of IFN-γ treatment after a single injection in non-responders. However, this approach should be tested in future trials before implementation.

Supplementary Information

The online version contains supplementary material available at https://doi.org/10.1186/s13054-026-05946-6.

Additional file 1

Additional file 2

Additional file 3

Additional file 4

Additional file 5

Acknowledgements

We thank the biological resource center for biobanking of CHU Nantes (Hôtel Dieu, Centre de Ressources Biologiques, Nantes, F-44093, France, BRIF: BB-0033-00040). We thank the ATLANREA study group for providing access to its dataset. We thank Mrs Cecila Le Bel, Mrs Noelline Mathelier, Mrs Delphine Flattres Duchaussoy and Mr Flavien Counille for their help with data collection and technical assistance.

Author contributions

M.P., D.S., E.M. J.P. And A.R. selected studies, performed data analyses, interpreted results, and drafted the manuscript. F.P.M., C.P., D.F.D, D.K, L.F.B, A.T., included patients, managed samples, collected clinical data, and revised the manuscript. A.Z., L.H.N. and A.V.F performed experiments and A.Z., B.N., J.H.A.M. and M.N. performed data analyses, interpreted results and revised the manuscript. All authors have approved the final manuscript for publication. No medical writer was involved in the preparation of this manuscript.

Funding

A.R. and A.T. received grant from European Union's Horizon 2020 research and innovation program under grant agreement number 847782 and Horizon Europe programme under grant agreement No 101137148., A.R. from the Agency National de la Recherche (ANR) PROGRAM project, and MSD avenir grant (Phenomenon project).

Data availability

Correspondence and requests should be addressed to A.R. (antoine.roquilly@univ-nantes.fr)

Code availability

All analyses were performed using publicly available software and published code as described in Methods.

Declarations

Ethics approval

The collection of human samples within IBIS has been declared to the French Ministry of Health (Programme de recherche "Immunologie", DC2014-2206, authorization renewed DC-2017-2987) and was approved by the Comité de Protection des Personnes Ouest IV (7/04/2015 and 08/10/2020, number clinicaltrial.gov NCT02003196). The CERAR (Ethics Committee for Anesthesiology and Intensive Care Research) approved this secondary analysis protocol under the reference number IRB 00010254 – 2020 - 041. The PREV-HAP study protocol was approved by the Ouest II Angers (France) Ethics Committee in March 2021. All patients or their legal representatives consented to the use of data and samples for this study, as appropriate under national legislation.

Consent for publication

All the authors revised the final manuscript version and approved its submission for publication.

Competing interests

The authors declare no competing interests.

Author details

[1]Center for Research in Transplantation and Translational Immunology, UMR 1064, Nantes Université, Inserm, CHU Nantes, Nantes F-44000, France
[2]Nantes Université, CHU Nantes, Service d'Anesthesie Réanimation, Nantes F-44000, France
[3]Department of Internal Medicine and Radboud Center for Infectious Diseases, Radboud University Medical Center, Nijmegen, The Netherlands
[4]Murdoch Children's Research Institute and Department of Paediatrics, University of Melbourne, Royal Children's Hospital, Parkville, Australia
[5]The Biomedical Research Institute of Murcia (IMIB-Pascual Parrilla), Murcia, Spain
[6]Department of Molecular Biology, Faculty of Science, Radboud University Nijmegen, Nijmegen, the Netherlands
[7]Critical Care Department, King's College Hospital NHS Foundation Trust, London, UK
[8]UQ Centre for Clinical Research (UQCCR), Faculty of Medicine, The University of Queensland, Brisbane, Australia
[9]CibeRes (Centro de Investigación Biomédica en Red de Enfermedades Respiratorias, 06/06/0028), Institut d'Investigacions Biomèdiques August Pi i Sunyer (IDIBAPS), Barcelona, Spain
[10]Department of Pulmonology, Thorax Institute, Hospital Clinic de Barcelona, Barcelona, Spain
[11]Department of Medicine, School of Medicine, University of Barcelona, Barcelona, Spain
[12]Service des urgences, Nantes Université, CHU Nantes, F-44000 Nantes, France
[13]Department of Immunology and Metabolism, Life and Medical Sciences Institute, University of Bonn, Bonn, Germany
[14]Department of Microbiology and Immunology, The University of Melbourne, The Peter Doherty Institute for Infection and Immunity, Melbourne VIC 3000, Australia

Received: 4 January 2026 / Accepted: 4 March 2026
Published online: 12 March 2026

References

1. Ricard J-D, Conti G, Boucherie M, Hormann C, Poelaert J, Quintel M, et al. A European survey of nosocomial infection control and hospital-acquired pneumonia prevention practices. J Infection. 2012;65:285–91. https://doi.org/10.1016/j.jinf.2012.06.016.
2. Garnier M, Constantin J-M, Heming N, Camous L, Ferré A, Razazi K, et al. Epidemiology, risk factors and prognosis of ventilator-associated pneumonia during severe COVID-19: Multicenter observational study across 149 European Intensive Care Units. Anaesth Crit Care Pain Med. 2023;42:101184. https://doi.org/10.1016/j.accpm.2022.101184.
3. Lagarde C, Bouras M, Floch RL, Hourmant Y, Grillot N, Bourdiol A, et al. A multifaceted strategy to optimize pharmacokinetics of antimicrobial therapy in patients with hospital-acquired infections—a monocentre quality improvement project. J Antimicrob Chemother. 2023;78:1378–85. https://doi.org/10.1093/jac/dkad094.
4. Poulain C, Launey Y, Bouras M, Lakhal K, Dargelos L, Crémet L, et al. Clinical evaluation of the BioFire Respiratory Pathogen Panel for the guidance of empirical antimicrobial therapy in critically ill patients with hospital-acquired pneumonia: A multicenter, quality improvement project. Anaesth Crit Care Pain Med. 2024;43:101353. https://doi.org/10.1016/j.accpm.2024.101353.
5. Roquilly A, Chanques G, Lasocki S, Foucrier A, Fermier B, Courson HD, et al. Implementation of French Recommendations for the Prevention and the Treatment of Hospital-acquired Pneumonia: A Cluster-randomized Trial. Clin Infect Dis. 2020;73:e1601–10. https://doi.org/10.1093/cid/ciaa1441.
6. Chaumette T, Cinotti R, Mollé A, Solomon P, Castain L, Fourgeux C, et al. Monocyte Signature Associated with Herpes Simplex Virus Reactivation and Neurological Recovery after Brain Injury. Am J Resp Crit Care. 2022;206:295–310. https://doi.org/10.1164/rccm.202110-2324oc.
7. Venet F, Monneret G. Advances in the understanding and treatment of sepsis-induced immunosuppression. Nat Rev Nephrol. 2017. https://doi.org/10.1038/nrneph.2017.165.
8. Rubio I, Osuchowski MF, Shankar-Hari M, Skirecki T, Winkler MS, Lachmann G, et al. Current gaps in sepsis immunology: new opportunities for translational research. Lancet Infect Dis. 2019;19:e422–36. https://doi.org/10.1016/s1473-3099(19)30567-5.
9. Giamarellos-Bourboulis EJ, Aschenbrenner AC, Bauer M, Bock C, Calandra T, Gat-Viks I, et al. The pathophysiology of sepsis and precision-medicine-based immunotherapy. Nat Immunol. 2024;25:19–28. https://doi.org/10.1038/s41590-023-01660-5.
10. Roquilly A, Francois B, Huet O, Launey Y, Lasocki S, Weiss E, et al. Interferon gamma-1b for the prevention of hospital-acquired pneumonia in critically ill patients: a phase 2, placebo-controlled randomized clinical trial. Intensiv Care Med. 2023;49:530–44. https://doi.org/10.1007/s00134-023-07065-0.
11. Martin FP, Poulain C, Mulier JH, Motos A, Gourain V, Ogan I, et al. Identification and validation of robust hospital-acquired pneumonia subphenotypes associated with all-cause mortality: a multi-cohort derivation and validation. Intensive Care Med. 2025;51:692–707. https://doi.org/10.1007/s00134-025-07884-3.
12. Thomas-Rüddel D, Giamarellos-Bourboulis E, Neumann C, Briegel J, Roquilly A, Annane D, et al. IFNγ in human sepsis: a scoping review. Ann Intensive Care. 2025;15:112. https://doi.org/10.1186/s13613-025-01534-z.
13. Montassier E, Kitsios GD, Radder JE, Bastard QL, Kelly BJ, Panzer A, et al. Robust airway microbiome signatures in acute respiratory failure and hospital-acquired pneumonia. Nat Med. 2023;29:2793–804. https://doi.org/10.1038/s41591-023-02617-9.
14. Roquilly A, Jacqueline C, Davieau M, Mollé A, Sadek A, Fourgeux C, et al. Alveolar macrophages are epigenetically altered after inflammation, leading to long-term lung immunoparalysis. Nat Immunol. 2020;21:636–48. https://doi.org/10.1038/s41590-020-0673-x.
15. Roquilly A, McWilliam HEG, Jacqueline C, Tian Z, Cinotti R, Rimbert M, et al. Local modulation of antigen-presenting cell development after resolution of pneumonia induces long-term susceptibility to secondary infections. Immunity. 2017;47:135-147.e5. https://doi.org/10.1016/j.immuni.2017.06.021.
16. Boomer JS, To K, Chang KC, Takasu O, Osborne DF, Walton AH, et al. Immunosuppression in patients who die of sepsis and multiple organ failure. JAMA. 2011;306:2594–605. https://doi.org/10.1001/jama.2011.1829.
17. Hotchkiss RS, Monneret G, Payen D. Sepsis-induced immunosuppression: from cellular dysfunctions to immunotherapy. Nat Rev Immunol. 2013. https://doi.org/10.1038/nri3552.
18. Cheng S-C, Scicluna BP, Arts RJW, Gresnigt MS, Lachmandas E, Giamarellos-Bourboulis EJ, et al. Broad defects in the energy metabolism of leukocytes underlie immunoparalysis in sepsis. Nat Immunol. 2016;17:406–13. https://doi.org/10.1038/ni.3398.
19. Cao S, Li H, Xin J, Jin Z, Zhang Z, Li J, et al. Identification of genetic profile and biomarkers involved in acute respiratory distress syndrome. Intensiv Care Med. 2023. https://doi.org/10.1007/s00134-023-07248-9.
20. Roquilly A, Torres A, Villadangos JA, Netea MG, Dickson R, Becher B, et al. Pathophysiological role of respiratory dysbiosis in hospital-acquired pneumonia. Lancet Respir Med. 2019;7:710–20. https://doi.org/10.1016/s2213-2600(19)30140-7.
21. Langelier C, Kalantar KL, Moazed F, Wilson MR, Crawford ED, Deiss T, et al. Integrating host response and unbiased microbe detection for lower respiratory tract infection diagnosis in critically ill adults. Proc Natl Acad Sci U S A. 2018;115:201809700. https://doi.org/10.1073/pnas.1809700115.

22. Antcliffe DB, Harte E, Hussain H, Jiménez B, Browning C, Gordon AC. Metabolic septic shock sub-phenotypes, stability over time and association with clinical outcome. Intensiv Care Med. 2025. https://doi.org/10.1007/s00134-025-07859-4.
23. Torres A, Niederman MS, Chastre J, Ewig S, Fernandez-Vandellos P, Hanberger H, et al. International ERS/ESICM/ESCMID/ALAT guidelines for the management of hospital-acquired pneumonia and ventilator-associated pneumonia: guidelines for the management of hospital-acquired pneumonia (HAP)/ventilator-associated pneumonia (VAP) of the European Respiratory Society (ERS), European Society of Intensive Care Medicine (ESICM), European Society of Clinical Microbiology and Infectious Diseases (ESCMID) and Asociación Latinoamericana del Tórax (ALAT). Eur Respir J. 2017;50:1700582. https://doi.org/10.1183/13993003.00582-2017.
24. Leone M, Bouadma L, Bouhemad B, Brissaud O, Dauger S, Gibot S, et al. Hospital-acquired pneumonia in ICU. Anaesth Crit Care Pain Med. 2018;37:83–98. https://doi.org/10.1016/j.accpm.2017.11.006.
25. Force ADT, Ranieri VM, Rubenfeld GD, Thompson BT, Ferguson ND, Caldwell E, et al. Acute Respiratory Distress Syndrome: The Berlin Definition. JAMA. 2012;307:2526–33. https://doi.org/10.1001/jama.2012.5669.
26. ARDS Definition Task Force, Ranieri VM, Rubenfeld GD, Thompson BT, Ferguson ND, Caldwell E, et al. Acute respiratory distress syndrome: the Berlin Definition. 2012;2526--2533.
27. Deininger S-O, Cornett DS, Paape R, Becker M, Pineau C, Rauser S, et al. Normalization in MALDI-TOF imaging datasets of proteins: practical considerations. Anal Bioanal Chem. 2011;401:167–81. https://doi.org/10.1007/s00216-011-4929-z.
28. Moorlag SJCFM, Folkman L, ter Horst R, Krausgruber T, Barreca D, Schuster LC, et al. Multi-omics analysis of innate and adaptive responses to BCG vaccination reveals epigenetic cell states that predict trained immunity. Immunity. 2024;57(1):171–87.
29. Ziogas A, Novakovic B, Ventriglia L, Galang N, Tran KA, Li W, et al. Long-term histone lactylation connects metabolic and epigenetic rewiring in innate immune memory. Cell. 2025;188:2992-3012.e16. https://doi.org/10.1016/j.cell.2025.03.048.
30. Hagenberg J, Budde M, Pandeva T, Kondofersky I, Schaupp SK, Theis FJ, et al. longmixr: a tool for robust clustering of high-dimensional cross-sectional and longitudinal variables of mixed data types. Bioinformatics. 2024. https://doi.org/10.1093/bioinformatics/btae137.
31. Zhang D, Tang Z, Huang H, Zhou G, Cui C, Weng Y, et al. Metabolic regulation of gene expression by histone lactylation. Nature. 2019;574:575–80. https://doi.org/10.1038/s41586-019-1678-1.
32. Weiss E, Zahar J-R, Alder J, Asehnoune K, Bassetti M, Bonten MJM, et al. Elaboration of Consensus Clinical Endpoints to Evaluate Antimicrobial Treatment Efficacy in Future Hospital-acquired/Ventilator-associated Bacterial Pneumonia Clinical Trials. Clin Infect Dis Official Publ Infect Dis Soc Am. 2019;69:1912–8. https://doi.org/10.1093/cid/ciz093.
33. Crowe NY, Smyth MJ, Godfrey DI. A Critical Role for Natural Killer T Cells in Immunosurveillance of Methylcholanthrene-induced Sarcomas. J Exp Medicine. 2002;196:119–27. https://doi.org/10.1084/jem.20020092.
34. Castón JJ, Cantisán S, González-Gasca F, Páez-Vega A, Abdel-Hadi H, Illescas S, et al. Interferon-γ production by CMV-specific CD8+ T lymphocytes provides protection against cytomegalovirus reactivation in critically ill patients. Intensiv Care Med. 2016;42:46–53. https://doi.org/10.1007/s00134-015-4077-6.
35. Payen D, Faivre V, Miatello J, Leentjens J, Brumpt C, Tissières P, et al. Multicentric experience with interferon gamma therapy in sepsis induced immunosuppression. A case series BMC Infect Dis. 2019;19:931. https://doi.org/10.1186/s12879-019-4526-x.
36. Kotsaki A, Pickkers P, Bauer M, Calandra T, Lupse M, Wiersinga WJ, et al. ImmunoSep (Personalised Immunotherapy in Sepsis) international double-blind, double-dummy, placebo-controlled randomised clinical trial: study protocol. BMJ Open. 2022;12:e067251. https://doi.org/10.1136/bmjopen-2022-067251.
37. Giamarellos-Bourboulis EJ, Antonelli M, Bloos F, Kotsamidi I, Psarrakis C, Dakou K, et al. Interferon-gamma driven elevation of CXCL9: a new sepsis endotype independently associated with mortality. EBioMedicine. 2024;109:105414. https://doi.org/10.1016/j.ebiom.2024.105414.
38. Leventogiannis K, Kyriazopoulou E, Antonakos N, Kotsaki A, Tsangaris I, Markopoulou D, et al. Toward personalized immunotherapy in sepsis: the PROVIDE randomized clinical trial. Cell Rep Med. 2022;3:100817. https://doi.org/10.1016/j.xcrm.2022.100817.
39. Wyngene LV, Vandewalle J, Libert C. Reprogramming of basic metabolic pathways in microbial sepsis: therapeutic targets at last? EMBO Mol Med. 2018. https://doi.org/10.15252/emmm.201708712
40. Andrei S, Meilhac O, Tymowski CD, Snauwaert A, Stern J, Robert T, et al. Relationship between high-density lipoprotein cholesterol (HDL-C) concentration and ventilator-associated pneumonia in ICU COVID-19 patients. Anaesth Crit Care Pain Med. 2025;44:101535. https://doi.org/10.1016/j.accpm.2025.101535.

Publisher's Note